iScience

CellPress
OPEN ACCESS

Article

The Alpine ibex (Capra ibex) gut microbiome, seasonal dynamics, and potential application in lignocellulose bioconversion

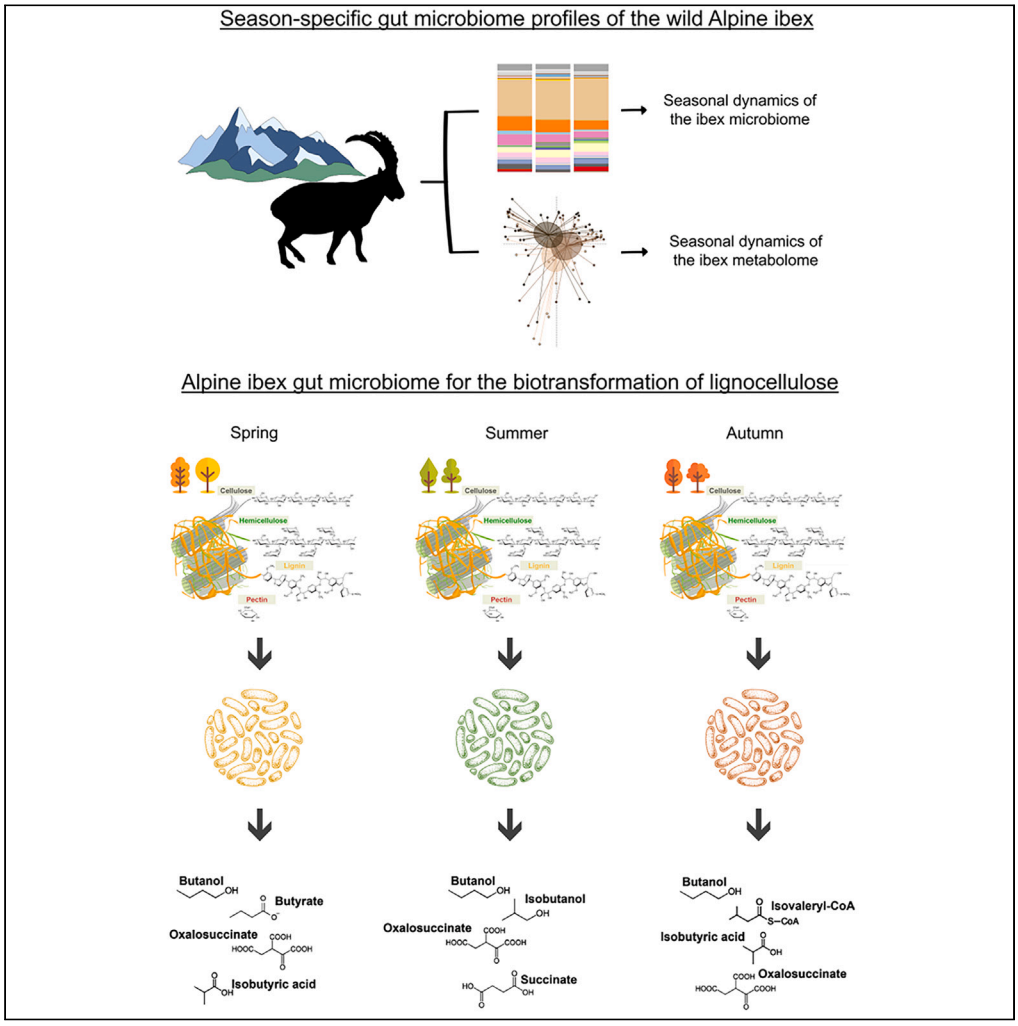

Enrico Nanetti, Daniel Scicchitano, Giorgia Palladino, ..., Jessica Fiori, Simone Rampelli, Marco Candela

marco.candela@unibo.it

Highlights

Season-specific profiles of *Alpine ibex (Capra ibex)* gut microbiome were identified

Gut microbiome provides Ibex with phenotypic plasticity to deal with seasonality

Thirty-eight species-level genome bins from the Ibex gut microbiome were identified

3 hubs for bioconversion of lignocellulosic biomasses to fatty acids were detected

Nanetti et al., iScience *27*, 110194
July 19, 2024
https://doi.org/10.1016/j.isci.2024.110194

iScience

CellPress
OPEN ACCESS

Article

The Alpine ibex (Capra ibex) gut microbiome, seasonal dynamics, and potential application in lignocellulose bioconversion

Enrico Nanetti,[1,10] Daniel Scicchitano,[1,2,10] Giorgia Palladino,[1,2] Nicolò Interino,[3] Luca Corlatti,[4,5] Luca Pedrotti,[4] Federica Zanetti,[6] Elena Pagani,[6] Erika Esposito,[3] Alice Brambilla,[7,8] Stefano Grignolio,[9] Ilaria Marotti,[6] Silvia Turroni,[1] Jessica Fiori,[3] Simone Rampelli,[1,2] and Marco Candela[1,2,11,*]

SUMMARY

Aiming to shed light on the biology of wild ruminants, we investigated the gut microbiome seasonal dynamics of the Alpine ibex (*Capra ibex*) from the Central Italian Alps. Feces were collected in spring, summer, and autumn during non-invasive sampling campaigns. Samples were analyzed by 16S rRNA amplicon sequencing, shotgun metagenomics, as well as targeted and untargeted metabolomics. Our findings revealed season-specific compositional and functional profiles of the ibex gut microbiome that may allow the host to adapt to seasonal changes in available forage, by fine-tuning the holobiont catabolic layout to fully exploit the available food. Besides confirming the importance of the host-associated microbiome in providing the phenotypic plasticity needed to buffer dietary changes, we obtained species-level genome bins and identified minimal gut microbiome community modules of 11–14 interacting strains as a possible microbiome-based solution for the bioconversion of lignocellulose to high-value compounds, such as volatile fatty acids.

INTRODUCTION

The gut microbiome is utterly recognized as a key element for host physiology, being involved in vital processes such as digestion, immunity, and protection.[1–3] Herbivorous mammals harbor complex and dynamic microbial communities in their guts, and ruminants are among the most studied animals for gut microbiome structure, dynamics, and functions.[4–6] Indeed, ruminants rely on gut symbionts (mainly bacteria, fungi, and protists) to break down the complex biopolymers of plant cell walls and extract energy from these dietary sources, making them an excellent model for investigating diet-host-microbiome relationships and dependencies.[5,7–9] However, while the cattle microbiome has been extensively studied[10–12]—also due to their high economic importance and role in the current global change scenario—less is known about the structure and function of microbiomes associated with wild ruminants, weakening our understanding of the full diversity and complexity of the ruminant gut microbiome and its importance in animal biology.[7,9,13] Also, wild ruminants consume a more complex and diverse diet than their domesticated relatives and are also more tolerant to roughage and lignin.[14,15] This makes their gut microbiome a possible, yet untapped, source of a diverse and undiscovered array of enzymes and taxa as a valuable natural reservoir of functionalities for the efficient digestion and valorization of lignocellulosic (LC) substrates.[16,17]

Recent research has suggested the importance of wild ruminants' gut microbiomes in cooperating with their hosts to cope with their complex and diverse wild plant-based diet.[8,9,15,18] However, studies were based on 16S rRNA amplicon sequencing, making it difficult to mechanistically understand the functional role of the gut microbiome in the adaptation to seasonal dietary shifts.

To shed light on this and to explore the potential of the ibex gut microbiome for industrial LC bioconversion processes, we collected fresh fecal samples from 86 wild individuals of Alpine ibex (*Capra ibex*). Fecal samples were chosen since they are recognized as a good (and non-invasive) proxy for microbial diversity across the ruminant digestive tract,[19] being possibly enriched in functionalities for degrading the most

[1]Unit of Microbiome Science and Biotechnology, Department of Pharmacy and Biotechnology (FaBiT), Alma Mater Studiorum - University of Bologna, Via Belmeloro 6, 40126 Bologna, Italy
[2]Fano Marine Center, The Inter-Institute Center for Research on Marine Biodiversity, Resources and Biotechnologies, 61032 Fano, Italy
[3]Department of Chemistry "G. Ciamician", University of Bologna, Via Selmi 2, 40126 Bologna, Italy
[4]Stelvio National Park, 23032 Bormio, Italy
[5]University of Freiburg, 79098 Freiburg, Germany
[6]Department of Agricultural and Food Sciences, University of Bologna, Viale G. Fanin 44, 40127 Bologna, Italy
[7]Department of Evolutionary Biology and Environmental Studies, University of Zurich, Winterthurerstrasse 190, 8057 Zurich (CH), Switzerland
[8]Centro Studi Fauna Alpina, Parco Nazionale Gran Paradiso, Loc. Degioz 11, 11010 Valsavarenche, Aosta, Italy
[9]University of Ferrara, Department of Life Science and Biotechnology, via Borsari 46, I-44121 Ferrara, Italy
[10]These authors contributed equally
[11]Lead contact
*Correspondence: marco.candela@unibo.it
https://doi.org/10.1016/j.isci.2024.110194

recalcitrant and indigestible portion of the plant food, as it is not completely processed in the foregut. Among large ruminant mammals, the Alpine ibex is the species using areas located at the highest elevations[20] of the Alps, where seasonality is pronounced, with a long winter season and low availability of forage that alternates with a late spring-summer season with high availability of good-quality forage. As a result, spatial behavior and habitat selection clearly vary among the seasons, as well as diet.[21–23] This makes the Alpine ibex an excellent case study for investigating the responses of the microbiome to the seasonality of trophic resources, including roughage or available trees and bushes, which would require the selection of specialized gut microbiome components for the digestion of more recalcitrant plant foods. Sampling was performed across 3 different seasons, namely spring (June 2020), summer (August 2020), and fall (October 2020), at the Stelvio National Park, Lombardia (Italy). Samples were collected from animals of approximately the same age, sampled non-invasively by actively searching for animals over 2–3 days and waiting for fecal deposition. Samples were then analyzed by multiomics (i.e., 16S rRNA amplicon sequencing, shotgun metagenomics, and metabolomics), in an attempt to map the compositional and functional shifts of the ibex gut microbiome in response to seasonal vegetation changes from spring to fall. Our results showed well-defined seasonal dynamics of the Alpine ibex gut microbiome, with community modules, taxa, functions, and metabolites characterized by clear seasonal patterns. While providing some glimpses on the importance of the gut microbiome for the ibex biology, we discovered new microorganisms and community modules as potential candidates for biotechnological processes of LC bioconversion and valorization.

RESULTS

Seasonal variation in the compositional structure of the Alpine ibex gut microbiome

A total of 86 Alpine ibex feces, 17 soil, and 8 grass samples were collected from two different sites (i.e., "Passo del Gavia" and "Valle del Braulio") at Stelvio National Park, Lombardia (Italy), in June, August, and October 2020 (see Figure S1 for sampling coordinates and normalized difference vegetation index of the sampling area for each sampling season). In particular, we collected approximately the same number of ibex samples from each site and season to obtain a comparable subset of animal data for the three selected seasons (see Table S1 for sampling details). The vegetation map of sampling sites highlighted that the majority of species grouped into the Magnoliophyta division, whereas the remaining species belonged to the Pinophyta division. Based on Raunkiaer's classification, plants occurred mostly as hemicryptophytes (48%), followed by chamaephytes (7%), phanerophytes (5%), geophytes (5%), and therophytes (2%). Snow on the ground (cm) from 1992 to 2020 is provided in Figure S2, and 2019–2020 showed one of the highest records in the period of observation.

For microbiome analysis, we performed bacterial metabarcoding (i.e., 16S rRNA gene sequencing of the V3-V4 hypervariable regions), shotgun metagenomics, and metabolomics. First, a Bray-Curtis-based principal coordinates analysis (PCoA) of the 16S rRNA gene-based taxonomic composition of the entire set of 111 samples (ibex, soil, and grass) was performed. Data revealed three distinct clusters matching the three ecosystem types (permutation test with pseudo-F ratio, $p = 0.001$), with the soil microbiome showing the highest alpha diversity, followed by the Alpine ibex gut microbiome and then by the grass microbiome (Kruskal-Wallis test, $p \leq 0.001$) (Figure S3). As no separation was observed between the ibex gut microbiome profiles of the two sampling areas (permutation test with pseudo-F ratio, $p = 0.66$), the two Alpine ibex subpopulations were considered as one for subsequent analyses. Indeed, the Valle del Braulio and Passo del Gavia ibex colonies share the same genetic origin, and, since the exchange of individuals between the colonies cannot be excluded, although limited in number, the two colonies can be regarded as a single meta-population.[24,25]

At the phylum level, the Alpine ibex gut microbiome was characterized by two dominant phyla, namely Firmicutes (mean relative abundance ±SD, 62.8% ± 13.2%) and Bacteroidetes (19.6% ± 8.5%). Actinobacteria (6.2% ± 8.0%), Saccharibacteria (3.8% ± 4.2%), Verrucomicrobia (3.0% ± 2.9%), and Proteobacteria (2.6% ± 5.9%) were less abundant phyla. At the family level, the dominant taxa were *Ruminococcaceae* (35.8% ± 14.1%), *Lachnospiraceae* (11.0% ± 4.3%), and *Christensenellaceae* (7.6% ± 3.4%). Subdominant families were *Rikenellaceae* (6.7% ± 3.8%), *Bacteroidaceae* (4.2% ± 3.0%), *Prevotellaceae* (4.0% ± 3.5%), and *Coriobacteriaceae* (3.2% ± 3.8%). For the phylum- and family-level bacterial composition of the Alpine ibex gut microbiome across seasons, see Figure S4.

Notably, the ibex gut microbiomes clearly segregated by season in the Bray-Curtis-based PCoA (permutation test with pseudo-F ratio, $p = 0.001$) (Figure 1A). Conversely, no significant differences were found when comparing alpha diversity across seasons (Kruskal-Wallis test, $p > 0.05$) (Figure 1B). According to Linear discriminant analysis Effect Size (LEfSe) analysis[68] (Figure 1C), genera associated with spring were *Christensenellaceae R-7* group, *Ruminococcaceae NK4A214* group, *FamilyXIII AD3011* group, *Lachnospiraceae NK3A20* group, *Ruminococcus 2*, *Eubacterium hallii* group, *Streptococcus*, *Eubacterium nodatum* group, *Acetitomaculum*, and *Chthoniobacter*. Summer samples were enriched in *Solibacillus* and *Prevotella 7*, while autumn samples in *Arthrobacter*, *Ruminococcaceae UCG-010*, *Bacillus*, *Paenibacillus*, *Pseudomonas*, *Paludibacter*, *Ruminiclostridium 1*, *Odoribacter*, and *Staphylococcus*. The only component of the core Alpine ibex gut microbiome identified in our dataset, defined as the only genus present with a relative abundance ≥3% in at least 75% of the samples in each season,[26] was *Christensenellaceae R-7* group.

Seasonal changes in the Alpine ibex gut microbiome functional repertoire and metabolome

On a selected and representative subset of 12 Alpine ibex gut microbiome samples, 4 for each season, shotgun metagenomics was carried out, obtaining an average of 5.2 ± 1.0 million high-quality reads per sample. According to the PCoA based on Bray-Curtis distances between the abundance patterns of knockout (KO) genes, there was a trend toward a sample segregation by season (permutation test with pseudo-F ratio, $p = 0.088$) (Figure 2A). Conversely, no changes in functional diversity were observed, with alpha-diversity scores remaining constant across seasons (Figure 2B).

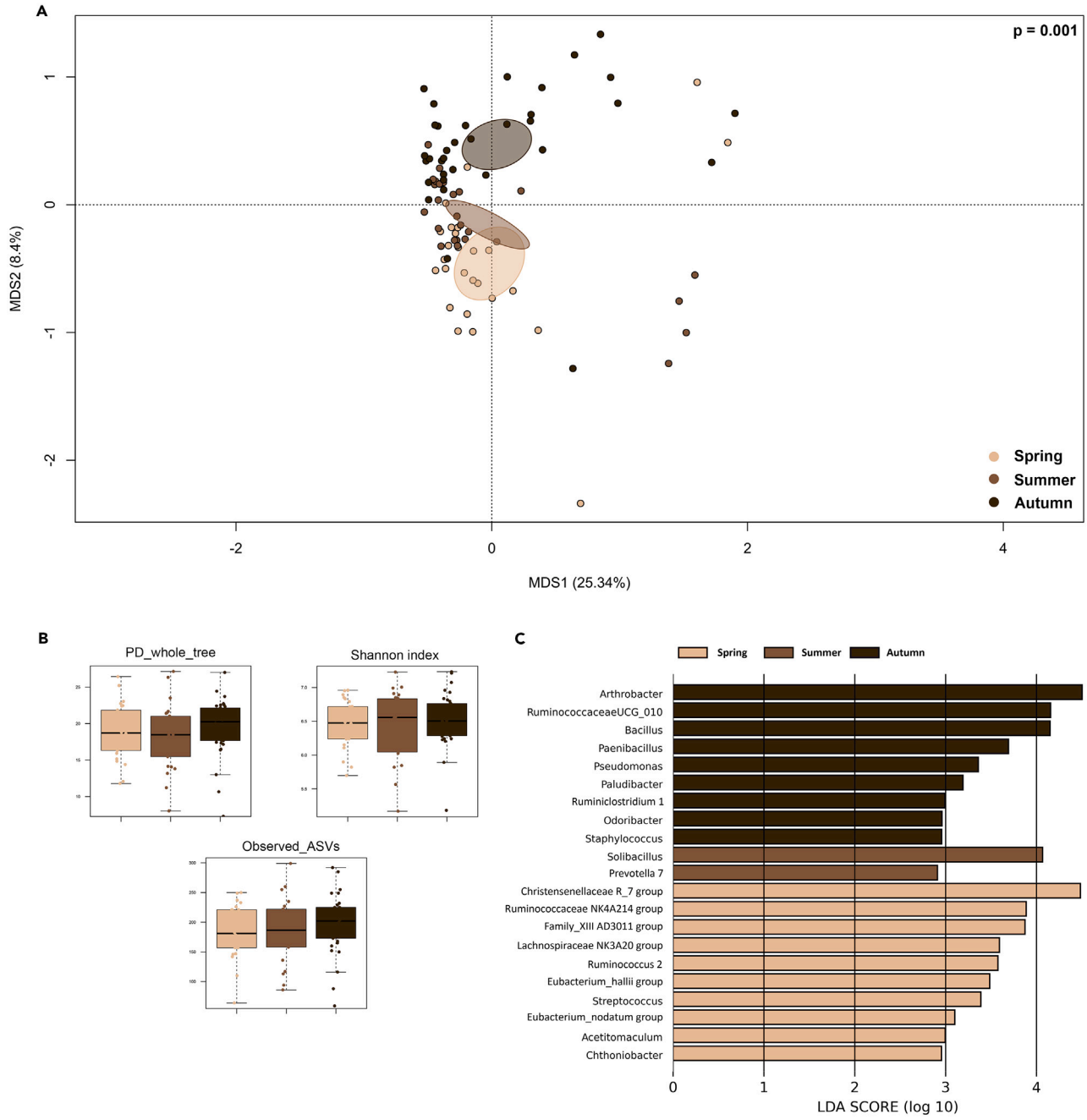

Figure 1. Seasonal variation of the compositional profile of the Alpine ibex gut microbiome

(A) Principal coordinates analysis (PCoA) based on Bray-Curtis distances between the Alpine ibex gut microbiome profiles across seasons, i.e., spring (June, light brown), summer (August, brown), and autumn (October, dark brown) (permutation test with pseudo-F ratio, $p = 0.001$). The first and second principal components (MDS1 and MDS2) are plotted, and the percentage of variance in the dataset explained by each axis is shown. Ellipses include the 95% confidence area based on the standard error of the weighted average of samples coordinates.

(B) Boxplots showing the alpha-diversity distributions of the Alpine ibex gut microbiome in spring, summer, and autumn, based on the Faith's phylogenetic diversity (PD whole tree), the Shannon index, and the number of observed amplicon sequence variants (ASVs). No significant differences were found for any of the metrics (Kruskal-Wallis test, $p > 0.05$).

(C) Linear discriminant analysis (LDA) scores of discriminating Alpine ibex gut microbiome genera between spring, summer, and autumn (the logarithmic threshold for discriminating features was set to 2.0 with $p < 0.05$). Plots were obtained by LDA effect size (LEfSe) analysis.

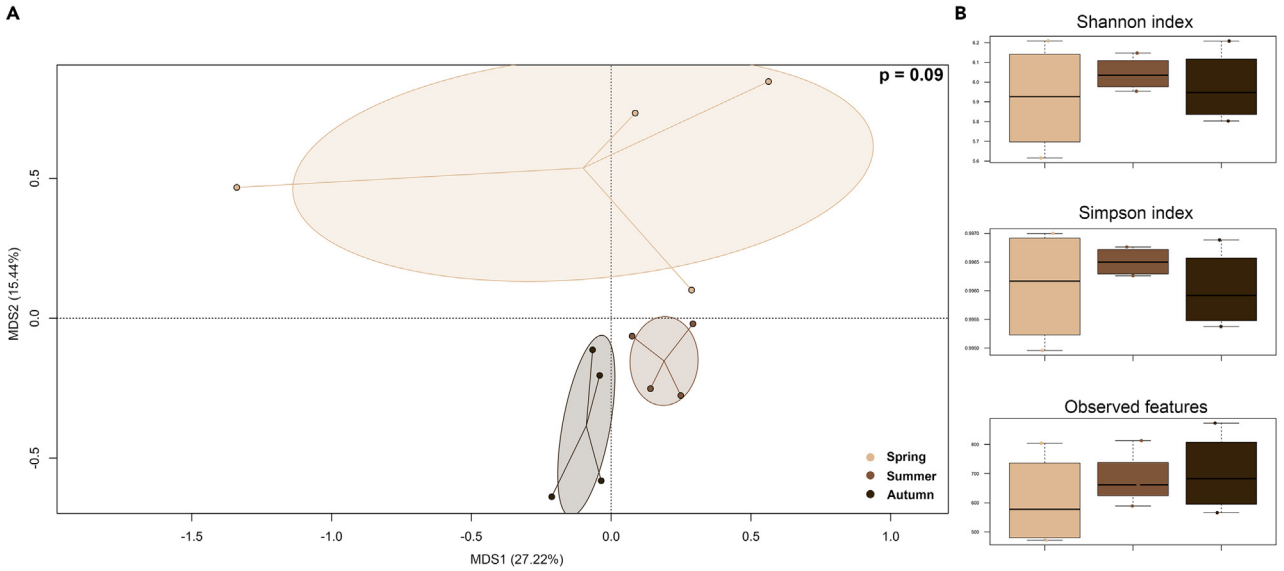

Figure 2. Seasonal variation of the functional profile of the Alpine ibex gut microbiome

(A) Principal coordinates analysis (PCoA) based on Bray-Curtis distances between Alpine ibex gut microbiome functional profiles of KO genes across seasons, i.e., spring (June, light brown), summer (August, brown), and autumn (October, dark brown) (permutation test with pseudo-F ratio, $p = 0.09$). The first and second principal components (MDS1 and MDS2) are plotted, and the percentage of variance in the dataset explained by each axis is shown. Ellipses include the 95% confidence area based on the standard error of the weighted average of samples coordinates.

(B) Boxplots showing the alpha-diversity distributions of the Alpine ibex gut microbiome functional profiles in spring, summer, and autumn, based on the Shannon index, the Simpson index, and the number of observed features. No significant differences were found for any of the metrics (Kruskal-Wallis test, $p > 0.05$).

Next, we focused on the Alpine ibex gut glycobiome, namely the set of Carbohydrate-Active enZYmes (CAZymes) encoded by the gut microbiome. Specifically, we identified 151 CAZymes in the ibex gut microbiome, representing all five classes listed in the CAZy database (http://www.cazy.org/Glycoside-Hydrolases.html), i.e., glycoside hydrolases (GHs), glycosyl transferases (GTs), polysaccharide lyases (PLs), carbohydrate esterases (CEs), and auxiliary activities (AAs). Notably, the ibex gut microbiome showed seasonal variations in the pattern of CAZymes involved in the catabolism of plant cell wall polysaccharides, including cellulases, xylanases, mannases, pectinases, β-glucosidases, and AAs enzymes (Figure 3). In particular, the autumn and summer samples were characterized by a higher load of cellulases, CEs, and β-glucosidases, while being depleted in auxiliary functions for lignin degradation, compared to the spring samples.

Finally, the entire set of Alpine ibex fecal samples ($n = 86$) was subjected to both targeted and untargeted metabolomics. According to our findings, the Alpine ibex gut metabolome, as assessed by untargeted metabolomics, showed a strong seasonal segregation ($p = 0.04$) (Figure 4A), which associated with the previously reported gut microbiome seasonal changes, as assessed by the procrustean randomized test ("protest," p value = 0.001 and correlation in a symmetrical rotation = 0.50). Similarly, we found relevant seasonal changes in the abundance profiles of the main short-chain fatty acids (SCFAs)/branched-chain fatty acids (BCFAs) in the ibex samples (Figure 4B). Specifically, a significant increase in acetic and isovaleric acid was observed in autumn compared to spring (Wilcoxon rank-sum test, $p \leq 0.05$), while a similar, but much smaller, trend was observed for valeric acid ($p = 0.06$), whereas propionic and butyric acid were significantly more abundant in spring and summer compared to autumn (Wilcoxon rank-sum test, $p < 0.01$).

Identification and characterization of SGB community modules from the Alpine ibex gut microbiome for the degradation of plant-derived biopolymers

Forty-nine high-quality metagenome-assembled genomes (MAGs) were obtained from the Alpine ibex gut microbiome and were successfully dereplicated into 38 species-level genome bins (SGBs). Only one of these SGBs (assigned to the *Acutalibacteraceae* family) showed a genetic distance <10% compared to already available genomes from ruminant gut microbiomes,[78] suggesting that the others could be unreported genomes. Notably, these 37 SGBs showed different distributions by season, as visualized in the PCoAs of the corresponding compositional profiles across the three different seasons, confirming the seasonal dynamics of the Alpine ibex gut microbiome also at the SGB level (Figure S5). Considering the SGB communities of the Alpine ibex gut microbiome characterizing each season, we next obtained the corresponding genome-scale metabolic models (GSMMs) for the degradation of the main plant components (namely cellulose, hemicellulose, lignin, and pectin) (Figure 5). Interestingly, for each season, we obtained a specific module of 11–14 SGBs synergistically interacting for the degradation of plant cell wall biopolymers (Table S2). Only three SGBs, belonging to *Akkermansia*, *Bacteroidaceae bacterium UBA4372*, and *Alistipes*, remained constant across all time points. Furthermore, based on the generated models, the primary metabolic endpoints from each SGB plant-degrading module were generally constant, with butanol and oxalosuccinate produced in all seasons, and isobutyric acid produced

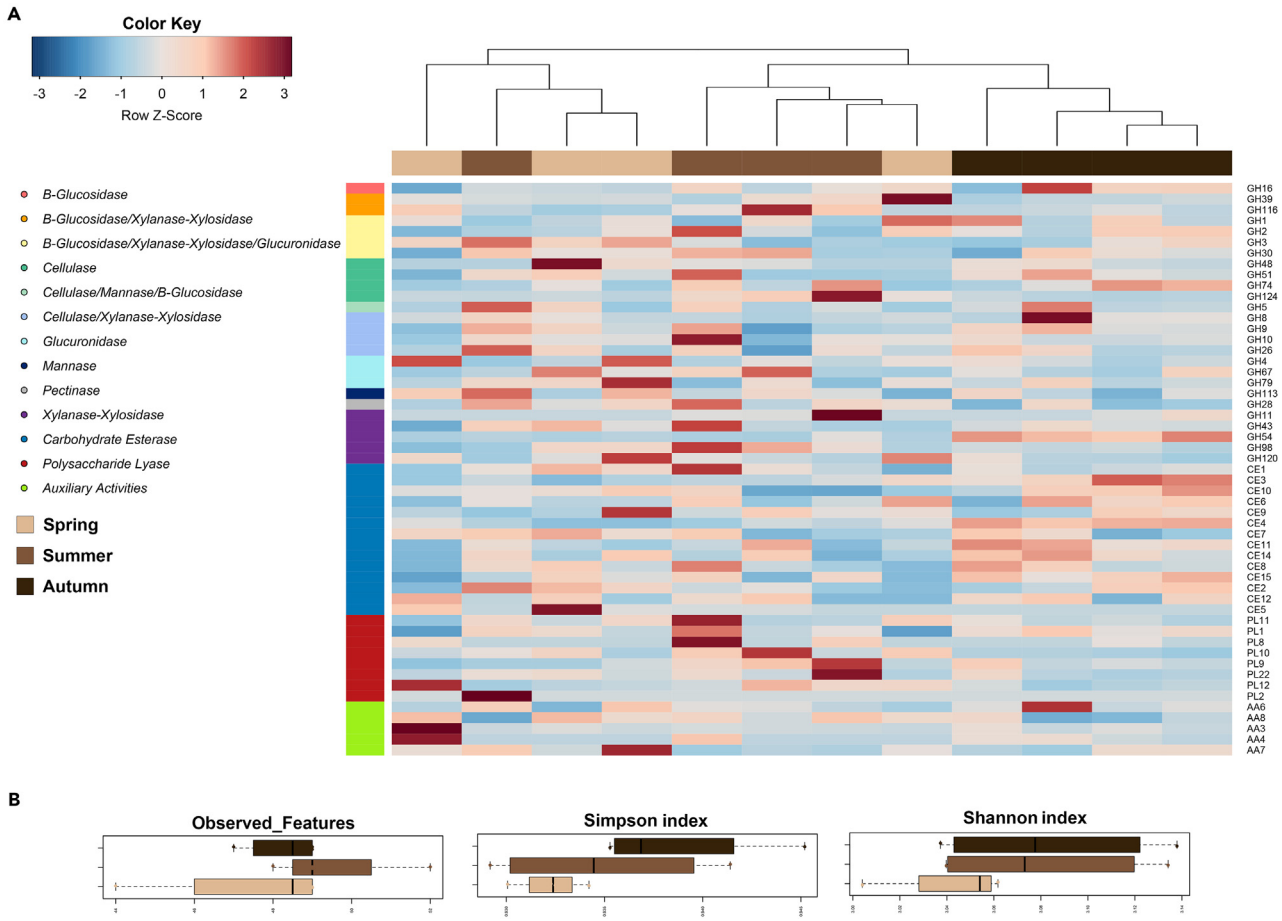

Figure 3. Seasonal variation of the glycobiome layout of the Alpine ibex gut microbiome

(A) Hierarchical Ward-linkage clustering based on the Spearman correlation coefficients of the reads per kilobase of gene per million reads mapped (RPKM) abundances of the main plant cell wall-hydrolyzing CAZymes families of the Alpine ibex gut microbiome across seasons, i.e., spring (June, light brown), summer (August, brown), and autumn (October, dark brown). The relative *Z* score is reported. Rows represent all CAZymes families grouped by the corresponding functional class.

(B) Boxplots showing the alpha-diversity distributions of CAZymes families of the Alpine ibex gut microbiome in spring, summer, and autumn, based on the number of observed features, the Simpson index, and the Shannon index. No significant differences were found for any of the metrics (Kruskal-Wallis test, $p > 0.05$).

in spring and autumn. In contrast, butyrate, isobutanol, succinate, and isovaleryl-coenzyme A (CoA) were season-specific metabolites (Figure 5).

DISCUSSION

According to our findings, the main phyla of the Alpine ibex gut microbiome were Firmicutes and Bacteroidetes, followed by Actinobacteria, Verrucomicrobia, and Saccharibacteria, while *Ruminococcaceae*, *Lachnospiraceae*, and *Christensenellaceae* were the dominant families. To the best of our knowledge, this is the first report on the bacterial fraction of the Alpine ibex gut microbiome, which to date has only been investigated considering fungal-methanogens associations[27] or targeting specific microbial pathogens.[28] Our results are consistent with those of the few available studies conducted on mountain ungulates, such as the long-tailed goral *Naemorhedus caudatus*,[29] mountain goats *Oreamnos americanus*,[7] takins *Budorcas taxicolor*,[30] and chamois *Rupicapra* spp.,[14,15] as well as on other wild and captive ruminants,[31–37] suggesting the presence of a phylogenetically widespread ruminant core gut microbiome at the family level. The fine multiomic assessment of the seasonal dynamics of the Alpine ibex gut microbiome allowed us to identify sharp seasonal patterns in terms of compositional, functional, and metabolic layouts. Notably, *Christensenellaceae R-7* group was detected as the only core microbiome genus (relative abundance $\geq$3% in at least 75% of the samples in each season), confirming the impressive seasonal changes in the Alpine ibex gut microbiome at low taxonomic ranks. On the other hand, as previously reported for other alpine ruminants,[35] no significant seasonal shifts were observed in alpha diversity, suggesting that a high level of microbial diversity is maintained throughout the year, possibly to ensure high redundancy in microbiome functionalities for digestion of available plants.

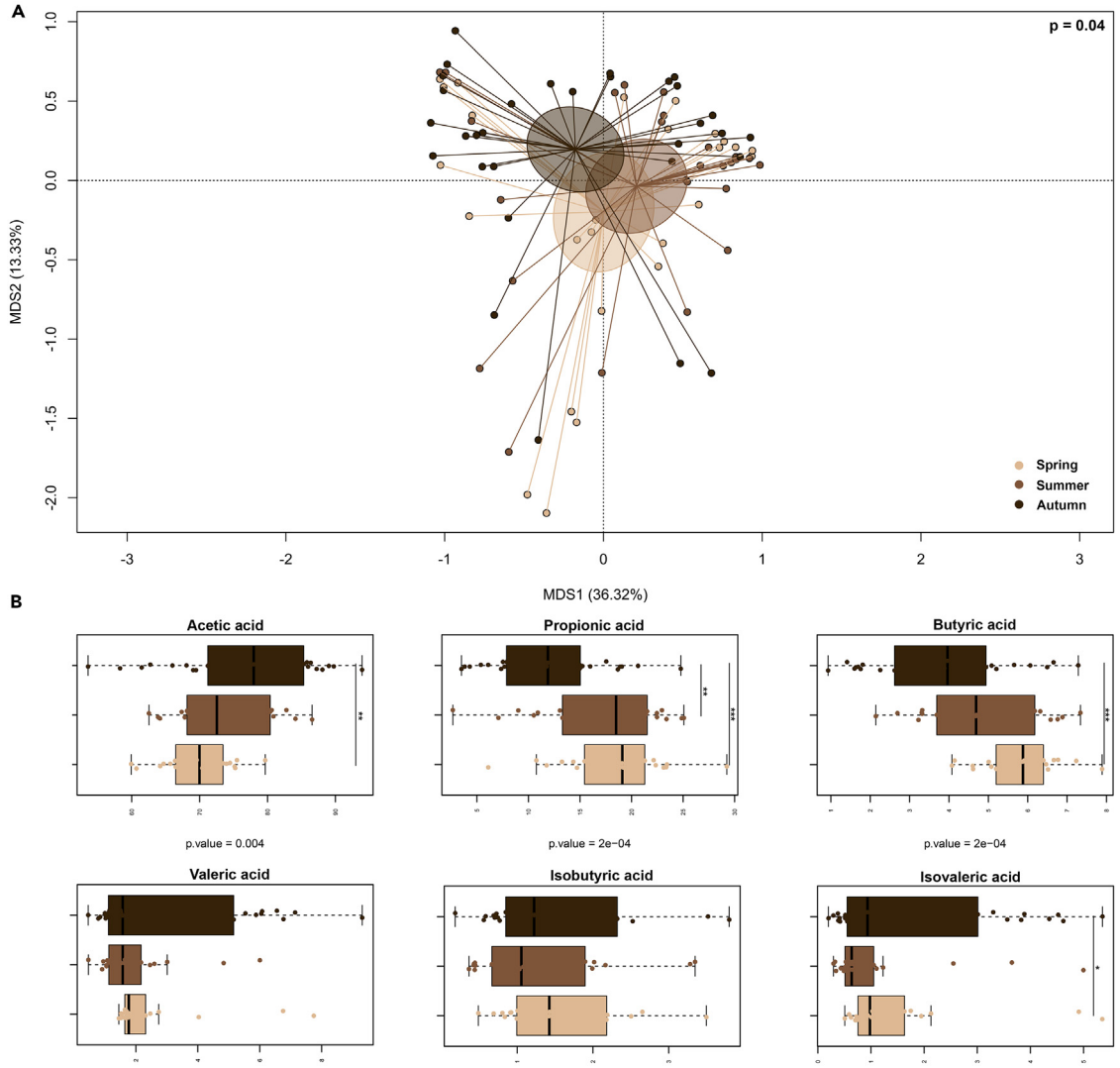

Figure 4. Seasonal variation of the Alpine ibex fecal metabolome

(A) Principal coordinates analysis (PCoA) based on Bray-Curtis distances between Alpine ibex fecal metabolomic profiles across seasons, i.e., spring (June, light brown), summer (August, brown), and autumn (October, dark brown) (permutation test with pseudo-F ratio, $p = 0.04$). The first and second principal components (MDS1 and MDS2) are plotted, and the percentage of variance in the dataset explained by each axis is shown. Ellipses include the 95% confidence area based on the standard error of the weighted average of samples coordinates.

(B) Boxplots showing the relative abundance distributions of short-chain fatty acids and branched-chain fatty acids in the Alpine ibex feces in spring, summer, and autumn. Kruskal-Wallis test and Wilcoxon rank-sum test controlled for multiple testing using false discovery rate (FDR); *p value $\leq$0.05; **p value $\leq$0.01; ***p value $\leq$0.001.

When we focused on the microbiome layout of CAZymes for the degradation of plant biopolymers to fermentable monosaccharides, we observed two distinct clusters according to the sampling season. In particular, one cluster was composed of summer and autumn samples enriched in CAZymes associated with a vast array of functionalities, such as cellulases, xylanases, PLs, CEs, and β-glucosidases, while the other cluster included spring samples, showing an overall lower diversity of CAZymes families, but a higher load of auxiliary enzymes dedicated to lignin oxidation and degradation. These results provide some insight into the mechanistic understanding of the functional importance of the Alpine ibex gut microbiome in the animal's adaptation to dietary shifts. More specifically, the studied year (2019–2020 period) was characterized by peculiar weather, which saw a prolonged persistence of snow on the ground until the beginning of June, with a direct effect on the available forage. Indeed, looking at the majority of the available plant species for the ibex (e.g., hemicryptophytes and geophytes), the snow sill on the ground in early June 2020 would have prevented their growth, and the ibex would have fed only on available trees and bushes, belonging to chamaephytes, phanerophytes, and therophytes, which are characterized by high lignin contents. In this condition, the Alpine ibex gut microbiome would respond adaptively, enriching for lignin-modifying functions, thus providing the host with the

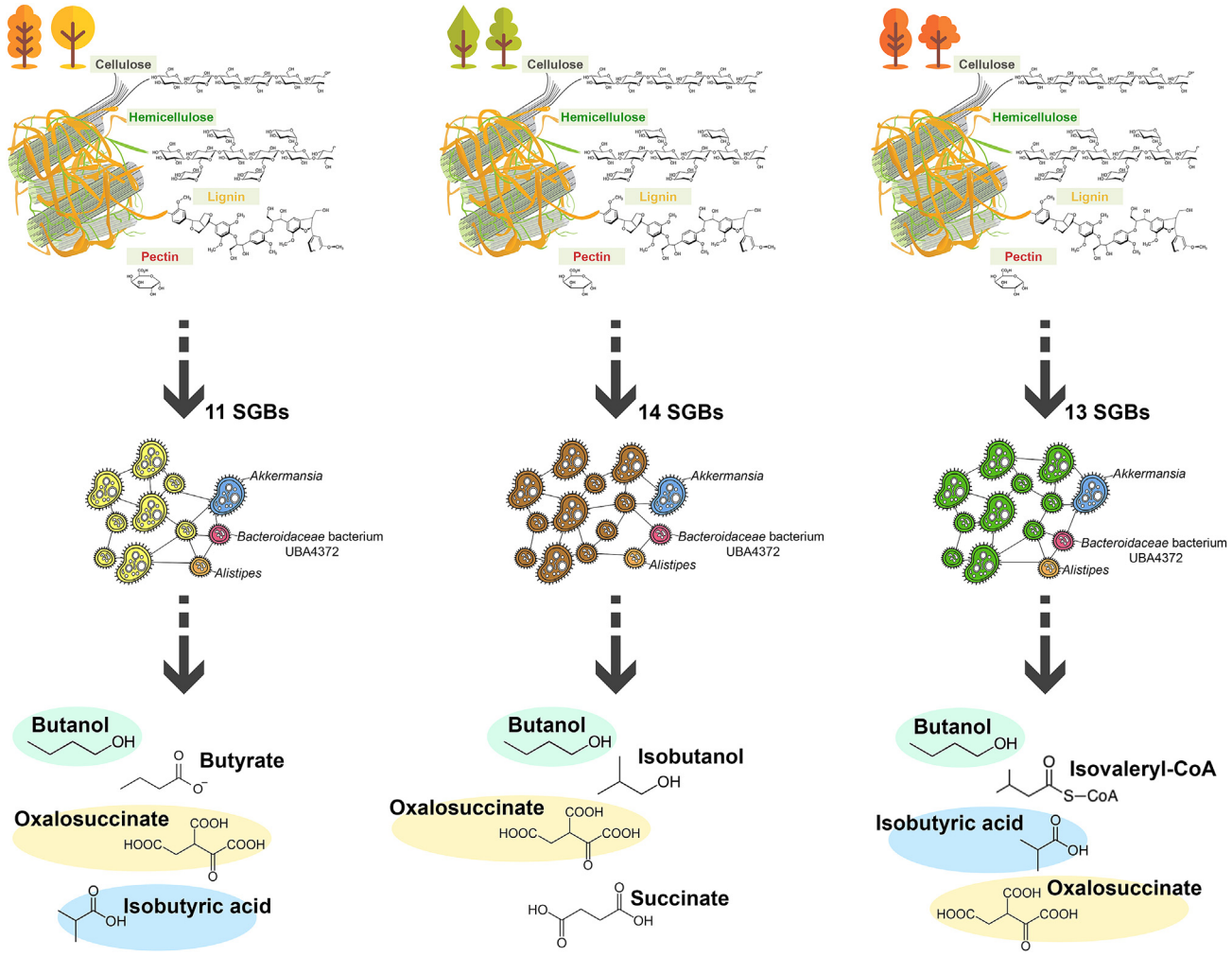

Figure 5. Seasonal genome-scale metabolic models of the Alpine ibex gut microbiome

Schematic representation of the main plant-derived biopolymers (top), the predicted SGB communities digesting such polymers (middle), and the resulting metabolic endpoints (bottom) in spring, summer, and autumn. Despite being largely characterized by different bacterial taxa, the ibex SGB gut communities appear to be able to ferment plant fibers and produce both common and unique endpoints depending on the season.

necessary degree of phenotypic plasticity to exploit this available plant food. On the contrary, the higher availability of grasses and herbs during the 2020 summer-autumn period would result in a diet enriched in cellulose and hemicellulose, with a concomitant decrease in total ingested lignin. Under these conditions, the Alpine ibex gut microbiome would respond by increasing the diversity of CAZymes for cellulose and hemicellulose degradation, allowing the full exploitation of the available dietary sources. This vision is also supported at the compositional level, as, in the summer period, the ibex gut microbiome was enriched in taxa belonging to *Prevotella 7*, whose members have been suggested to be among the most important protein, hemicellulose, and pectin degraders in ruminants.[38,39] Furthermore, autumn-enriched taxa included *Ruminococcaceae UCG-010*, *Bacillus*, *Paenibacillus*, *Pseudomonas*, and *Ruminiclostridium*, which have enhanced cellulose and hemicellulose digestion capabilities, via either secreted free enzymes or extracellular multi-enzyme structures called cellulosomes.[33,40–44] Interestingly, the seasonal changes in the Alpine ibex gut microbiome taxonomy would explain the corresponding shifts in the overall gut metabolome layout, as well as in the measured profiles of SCFAs. In particular, the higher levels of acetic acid in autumn may be due to the prevalence, in this season, of some well-known acetate producers such as *Ruminococcaceae UCG-010*,[33] *Ruminiclostridium*,[40] *Bacillus*,[45] and *Paenibacillus*.[46] Conversely, taxa such as *Eubacterium*, *Christensenellaceae*, *Prevotella*, and *Ruminococcus* may be correlated with increased proportions of propionic and butyric acid in spring and summer.[37,47–49] As the main endpoints of microbiome metabolism of plant biopolymers in the gut, SCFAs represent key molecules that support nutrition and regulate different aspects of animal physiology, including immune and metabolic homeostasis and protection against pathogenic microorganisms.[31,38,50] Although SCFAs are produced throughout the year, the Alpine ibex gut microbiome response to seasonal changes in available forage would also result in significant variation in their production profiles, raising concerns about the possible physiological importance of these changes in the holobiont metabolome. Finally, in

our study, SGBs and the related metabolic models were created, allowing the identification of season-specific Alpine ibex gut microbiome community modules for the degradation of plant biopolymers (i.e., cellulose, hemicellulose, lignin, and pectin) to alcohols and organic acids, including volatile fatty acids such as butyrate, isobutyrate, and isovaleryl-CoA. These minimal modules of 11–14 interacting strains may represent new candidate microbial consortia to be exploited in circular processes for the valorization of LC biomasses, enabling their bioconversion into value-added platform chemicals.[51] In addition, given the importance of transitioning to more sustainable and secure food systems, these community modules may foster innovative applications as next-generation probiotics in cattle, allowing for improved roughage tolerance in livestock for the transition to more sustainable farming strategies, with less reliance on green grasses, which require consistent amounts of water and are likely to be negatively affected by climate change.[52]

Overall, our findings support the importance of the Alpine ibex gut microbiome as a strategic evolutionary partner in the holobiont framework, providing the animal host with the necessary phenotypic plasticity to buffer seasonal changes in the available forage. This microbiome-host cooperation would be crucial for fine-tuning holobiont catabolism to fully exploit the available plant food. Besides confirming the relevance of the host-associated microbiome in the adaptation to dietary changes,[53,54] we provided some insight into the possible exploitation of the Alpine ibex gut microbiome for the development of innovative biotechnological solutions, in terms of circular LC bioconversion and valorization processes, and also as next-generation probiotics for the transition to more sustainable and secure food systems.

Limitations of the study

The main limit of our study is the lack of individual records of animal behavior and diet during the period of the study, which can be obtained by using GPS collars for animal tracking. Further, a second limitation is the lack of a second year of sampling, allowing to control for a possible annual variation. Finally, putative lignocellulose-degrading strains and hubs have been only identified as metagenomic assembled genomes, without having microbial isolates.

STAR★METHODS

Detailed methods are provided in the online version of this paper and include the following:

- KEY RESOURCES TABLE
- RESOURCE AVAILABILITY
  - Lead contact
  - Materials availability
  - Data and code availability
- EXPERIMENTAL MODEL AND STUDY PARTICIPANT DETAILS
  - Shotgun metagenomes
- METHOD DETAILS
  - Study site and sampling procedure
  - Microbial DNA extraction, 16S rRNA amplification and sequencing
  - Metabarcoding bioinformatics and biostatistics
  - Shotgun metagenomics sequencing
  - Metagenomics bioinformatics and biostatistics
  - Metagenome-Assembled Genomes (MAGs) reconstruction
  - Genome-scale metabolic models for the degradation of plant food substrates
  - Metabolomics
  - Reagents, materials and solutions
  - HS-SPME GC-MS analysis for SCFAs and BCFAs
  - LC-HRMSMS untargeted metabolomics
  - Data analysis

SUPPLEMENTAL INFORMATION

Supplemental information can be found online at https://doi.org/10.1016/j.isci.2024.110194.

ACKNOWLEDGMENTS

This research was supported by the PON "Ricerca e Innovazione" 2014–2020 program.

This research received no specific grant from any funding agency in the public, commercial, or not-for-profit sectors.

AUTHOR CONTRIBUTIONS

L.C. and M.C.: conceptualization. E.N., D.S., N.I., L.C., F.Z., I.M., and J.F.: data curation, formal analysis. L.C., L.P., and M.C.: project administration, resources, supervision. E.N. and D.S.: visualization. E.N., D.S., and M.C.: writing – original draft. G.P., N.I., L.C., L.P., F.Z., E.P., E.E., A.B., S.G., I.M., S.T., J.F., and S.R.: writing – review and editing.

DECLARATION OF INTERESTS

The authors declare no competing interests.

Received: February 1, 2024
Revised: April 24, 2024
Accepted: June 3, 2024
Published: June 6, 2024

REFERENCES

1. Hooper, L.V., Littman, D.R., and Macpherson, A.J. (2012). Interactions between the microbiota and the immune system. science *336*, 1268–1273. https://doi.org/10.1126/science.1223490.
2. McFall-Ngai, M., Hadfield, M.G., Bosch, T.C.G., Carey, H.V., Domazet-Lošo, T., Douglas, A.E., Dubilier, N., Eberl, G., Fukami, T., Gilbert, S.F., et al. (2013). Animals in a bacterial world, a new imperative for the life sciences. Proc. Natl. Acad. Sci. USA *110*, 3229–3236. https://doi.org/10.1073/pnas.1218525110.
3. Lindsay, E.C., Metcalfe, N.B., and Llewellyn, M.S. (2020). The potential role of the gut microbiota in shaping host energetics and metabolic rate. J. Anim. Ecol. *89*, 2415–2426. https://doi.org/10.1111/1365-2656.13327.
4. Huws, S.A., Creevey, C.J., Oyama, L.B., Mizrahi, I., Denman, S.E., Popova, M., Muñoz-Tamayo, R., Forano, E., Waters, S.M., Hess, M., et al. (2018). Addressing global ruminant agricultural challenges through understanding the rumen microbiome: past, present, and future. Front. Microbiol. *9*, 2161. https://doi.org/10.3389/fmicb.2018.02161.
5. Mizrahi, I., Wallace, R.J., and Moraïs, S. (2021). The rumen microbiome: balancing food security and environmental impacts. Nat. Rev. Microbiol. *19*, 553–566. https://doi.org/10.1038/s41579-021-00543-6.
6. Alessandri, G., Rizzo, S.M., Ossiprandi, M.C., van Sinderen, D., and Ventura, M. (2022). Creating an atlas to visualize the biodiversity of the mammalian gut microbiota. Curr. Opin. Biotechnol. *73*, 28–33. https://doi.org/10.1016/j.copbio.2021.06.028.
7. Haworth, S.E., White, K.S., Côté, S.D., and Shafer, A.B.A. (2019). Space, time and captivity: quantifying the factors influencing the fecal microbiome of an alpine ungulate. FEMS Microbiol. Ecol. *95*, fiz095. https://doi.org/10.1093/femsec/fiz095.
8. Eddington, H.S., Carroll, C., Larsen, R.T., McMillan, B.R., and Chaston, J.M. (2021). Spatiotemporal variation in the fecal microbiota of mule deer is associated with proximate and future measures of host health. BMC Vet. Res. *17*, 258. https://doi.org/10.1186/s12917-021-02972-0.
9. Su, R., Dalai, M., Luvsantseren, B., Chimedtseren, C., and Hasi, S. (2022). Comparative study of the function and structure of the gut microbiota in Siberian musk deer and Forest musk deer. Appl. Microbiol. Biotechnol. *106*, 6799–6817. https://doi.org/10.1007/s00253-022-12158-9.
10. Seshadri, R., Leahy, S.C., Attwood, G.T., Teh, K.H., Lambie, S.C., Cookson, A.L., Eloe-Fadrosh, E.A., Pavlopoulos, G.A., Hadjithomas, M., Varghese, N.J., et al. (2018). Cultivation and sequencing of rumen microbiome members from the Hungate1000 Collection. Nat. Biotechnol. *36*, 359–367. https://doi.org/10.1038/nbt.4110.
11. Wallace, R.J., Sasson, G., Garnsworthy, P.C., Tapio, I., Gregson, E., Bani, P., Huhtanen, P., Bayat, A.R., Strozzi, F., Biscarini, F., et al. (2019). A heritable subset of the core rumen microbiome dictates dairy cow productivity and emissions. Sci. Adv. *5*, eaav8391. https://doi.org/10.1126/sciadv.aav8391.
12. Furman, O., Shenhav, L., Sasson, G., Kokou, F., Honig, H., Jacoby, S., Hertz, T., Cordero, O.X., Halperin, E., Mizrahi, I., and Mizrahi, I. (2020). Stochasticity constrained by deterministic effects of diet and age drive rumen microbiome assembly dynamics. Nat. Commun. *11*, 1904. https://doi.org/10.1038/s41467-020-15652-8.
13. Jiang, F., Song, P., Wang, H., Zhang, J., Liu, D., Cai, Z., Gao, H., Chi, X., Zhang, T., and Zhang, T. (2022). Comparative analysis of gut microbial composition and potential functions in captive forest and alpine musk deer. Appl. Microbiol. Biotechnol. *106*, 1325–1339. https://doi.org/10.1007/s00253-022-11775-8.
14. Smoglica, C., Angelucci, S., Farooq, M., Antonucci, A., Marsilio, F., and Di Francesco, C.E. (2022). Microbial community and antimicrobial resistance in fecal samples from wild and domestic ruminants in Maiella National Park, Italy. One Health *15*, 100403.
15. Dahl, S.-A., Seifert, J., Camarinha-Silva, A., Hernández-Arriaga, A., Windisch, W., and König, A. (2023). "Get the best out of what comes in"–adaptation of the microbiota of chamois (Rupicapra rupicapra) to seasonal forage availability in the Bavarian Alps. Front. Microbiol. *14*, 1238744. https://doi.org/10.1016/j.onehlt.2022.100403.
16. Glendinning, L., Genç, B., Wallace, R.J., and Watson, M. (2021). Metagenomic analysis of the cow, sheep, reindeer and red deer rumen. Sci. Rep. *11*, 1990. https://doi.org/10.1038/s41598-021-81668-9.
17. Zhong, H., Zhou, J., Wang, F., Wu, W., Abdelrahman, M., and Li, X. (2022). Whole-genome sequencing reveals lignin-degrading capacity of a ligninolytic bacterium (Bacillus cereus) from Buffalo (Bubalus bubalis) rumen. Genes *13*, 842. https://doi.org/10.3390/genes13050842.
18. Couch, C.E., Stagaman, K., Spaan, R.S., Combrink, H.J., Sharpton, T.J., Beechler, B.R., and Jolles, A.E. (2021). Diet and gut microbiome enterotype are associated at the population level in African buffalo. Nat. Commun. *12*, 2267. https://doi.org/10.1038/s41467-021-22510-8.
19. Peng, X., Wilken, S.E., Lankiewicz, T.S., Gilmore, S.P., Brown, J.L., Henske, J.K., Swift, C.L., Salamov, A., Barry, K., Grigoriev, I.V., et al. (2021). Genomic and functional analyses of fungal and bacterial consortia that enable lignocellulose breakdown in goat gut microbiomes. Nat. Microbiol. *6*, 499–511. https://doi.org/10.1038/s41564-020-00861-0.
20. Parrini, F., Grignolio, S., Luccarini, S., Bassano, B., and Apollonio, M. (2003). Spatial behaviour of adult male Alpine ibex Capra ibex ibex in the Gran Paradiso National Park, Italy. Acta Theriol. *48*, 411–423. https://doi.org/10.1007/BF03194179.
21. Grignolio, S., Parrini, F., Bassano, B., Luccarini, S., and Apollonio, M. (2003). Habitat selection in adult males of Alpine ibex. Capra ibex ibex. FOLIA ZOOLOGICA-PRAHA- *52*, 113–120.
22. Grignolio, S., Rossi, I., Bassano, B., Parrini, F., and Apollonio, M. (2004). Seasonal variations of spatial behaviour in female Alpine ibex (Capra ibex ibex) in relation to climatic conditions and age. Ethology Ecology & Evolution *16*, 255–264. https://doi.org/10.1080/08927014.2004.9522636.
23. Brambilla, A., Bassano, B., Biebach, I., Bollmann, K., Keller, L., Toïgo, C., and von Hardenberg, A. (2022). Alpine Ibex Capra ibex Linnaeus, 1758. In Handbook of the Mammals of Europe (Springer International Publishing), pp. 1–27. https://doi.org/10.1007/978-3-319-65038-8_32-1.
24. M. Carro, and L. Pedrotti, eds. (2010). Atlante Parco nazionale dello Stelvio (Parco nazionale dello Stelvio).
25. Tosi, G. (2012). Lo stambecco in Lombardia e sull'arco alpino. Oikos.
26. Neu, A.T., Allen, E.E., and Roy, K. (2021). Defining and quantifying the core microbiome: challenges and prospects. Proc. Natl. Acad. Sci. USA *118*, e2104429118. https://doi.org/10.1073/pnas.2104429118.
27. Leis, S., Dresch, P., Peintner, U., Fliegerová, K., Sandbichler, A.M., Insam, H., and Podmirseg, S.M. (2014). Finding a robust strain for biomethanation: anaerobic fungi (Neocallimastigomycota) from the Alpine ibex (Capra ibex) and their associated methanogens. Anaerobe *29*, 34–43. https://doi.org/10.1016/j.anaerobe.2013.12.002.
28. Parrini, F., Cain, J.W., and Krausman, P.R. (2009). Capra ibex (Artiodactyla: Bovidae). Mamm. Species *830*, 1–12. https://doi.org/10.1644/830.1.
29. Park, C.E., Cho, B.J., Kim, M.J., Park, H.C., and Shin, J.H. (2021). Geographical relationships between long-tailed goral (Naemorhedus caudatus) populations based on gut microbiome analysis. Microorganisms *9*, 2002. https://doi.org/10.3390/microorganisms9092002.
30. Chen, J., Zhang, H., Wu, X., Shang, S., Yan, J., Chen, Y., Zhang, H., Tang, X., and Tang, X. (2017). Characterization of the gut microbiota in the golden takin (Budorcas taxicolor bedfordi). Amb. Express *7*, 81. https://doi.org/10.1186/s13568-017-0374-5.
31. Sundset, M.A., Præsteng, K.E., Cann, I.K.O., Mathiesen, S.D., and Mackie, R.I. (2007). Novel rumen bacterial diversity in two geographically separated sub-species of

reindeer. Microb. Ecol. *54*, 424–438. https://doi.org/10.1007/s00248-007-9254-x.
32. Cunha, I.S., Barreto, C.C., Costa, O.Y.A., Bomfim, M.A., Castro, A.P., Kruger, R.H., and Quirino, B.F. (2011). Bacteria and Archaea community structure in the rumen microbiome of goats (Capra hircus) from the semiarid region of Brazil. Anaerobe *17*, 118–124. https://doi.org/10.1016/j.anaerobe.2011.04.018.
33. Oikonomou, G., Teixeira, A.G.V., Foditsch, C., Bicalho, M.L., Machado, V.S., and Bicalho, R.C. (2013). Fecal microbial diversity in pre-weaned dairy calves as described by pyrosequencing of metagenomic 16S rDNA. Associations of Faecalibacterium species with health and growth. PLoS One *8*, e63157. https://doi.org/10.1371/journal.pone.0063157.
34. Liu, C., Wu, H., Liu, S., Chai, S., Meng, Q., and Zhou, Z. (2019). Dynamic alterations in yak rumen bacteria community and metabolome characteristics in response to feed type. Front. Microbiol. *10*, 1116. https://doi.org/10.3389/fmicb.2019.01116.
35. Yang, C., Tsedan, G., Liu, Y., and Hou, F. (2020). Shrub coverage alters the rumen bacterial community of yaks (Bos grunniens) grazing in alpine meadows. J. Anim. Sci. Technol. *62*, 504–520. https://doi.org/10.5187/jast.2020.62.4.504.
36. Fan, Q., Cui, X., Wang, Z., Chang, S., Wanapat, M., Yan, T., and Hou, F. (2021). Rumen microbiota of Tibetan sheep (Ovis aries) adaptation to extremely cold season on the Qinghai-Tibetan Plateau. Front. Vet. Sci. *8*, 673822. https://doi.org/10.3389/fvets.2021.673822.
37. Li, B., Jia, G., Wen, D., Zhao, X., Zhang, J., Xu, Q., Zhao, X., Jiang, N., Liu, Z., Wang, Y., and Wang, Y. (2022). Rumen microbiota of indigenous and introduced ruminants and their adaptation to the Qinghai–Tibetan plateau. Front. Microbiol. *13*, 1027138. https://doi.org/10.3389/fmicb.2022.1027138.
38. Dao, T.K., Do, T.H., Le, N.G., Nguyen, H.D., Nguyen, T.Q., Le, T.T.H., and Truong, N.H. (2021). Understanding the role of prevotella genus in the digestion of lignocellulose and other substrates in Vietnamese native goats' rumen by metagenomic deep sequencing. Animals. *11*, 3257. https://doi.org/10.3390/ani11113257.
39. Betancur-Murillo, C.L., Aguilar-Marín, S.B., and Jovel, J. (2022). Prevotella: A key player in ruminal metabolism. Microorganisms *11*, 1. https://doi.org/10.3390/microorganisms11010001.
40. Wang, C.M., Shyu, C.L., Ho, S.P., and Chiou, S.H. (2008). Characterization of a novel thermophilic, cellulose-degrading bacterium Paenibacillus sp. strain B39. Lett. Appl. Microbiol. *47*, 46–53. https://doi.org/10.1111/j.1472-765X.2008.02385.x.
41. Ravachol, J., Borne, R., Meynial-Salles, I., Soucaille, P., Pagès, S., Tardif, C., and Fierobe, H.P. (2015). Combining free and aggregated cellulolytic systems in the cellulosome-producing bacterium Ruminiclostridium cellulolyticum. Biotechnol. Biofuels *8*, 114. https://doi.org/10.1186/s13068-015-0301-4.
42. Guo, B., Li, D., Zhou, B., Jiang, Y., Bai, H., Zhang, Y., Xu, Q., Zhao, W., Chen, G., and Chen, G. (2019). Comparative characterization of bacterial communities in geese consuming of different proportions of ryegrass. PLoS One *14*, e0223445. https://doi.org/10.1371/journal.pone.0223445.
43. Qian, W., Ao, W., Jia, C., and Li, Z. (2019). Bacterial colonisation of reeds and cottonseed hulls in the rumen of Tarim red deer (Cervus elaphus yarkandensis). Antonie Leeuwenhoek *112*, 1283–1296. https://doi.org/10.1007/s10482-019-01260-0.
44. Sun, S., Zhang, Y., Liu, K., Chen, X., Jiang, C., Huang, M., Zang, H., Li, C., and Li, C. (2020). Insight into biodegradation of cellulose by psychrotrophic bacterium Pseudomonas sp. LKR-1 from the cold region of China: optimization of cold-active cellulase production and the associated degradation pathways. Cellulose *27*, 315–333. https://doi.org/10.1007/s10570-019-02798-y.
45. Speck, E.L., and Freese, E. (1973). Control of metabolite secretion in Bacillus subtilis. Microbiology *78*, 261–275. https://doi.org/10.1099/00221287-78-2-261.
46. Marwoto, B., Nakashimada, Y., Kakizono, T., and Nishio, N. (2004). Metabolic analysis of acetate accumulation during xylose consumption by Paenibacillus polymyxa. Appl. Microbiol. Biotechnol. *64*, 112–119. https://doi.org/10.1007/s00253-003-1435-z.
47. Pascal, V., Pozuelo, M., Borruel, N., Casellas, F., Campos, D., Santiago, A., Martinez, X., Varela, E., Sarrabayrouse, G., Machiels, K., et al. (2017). A microbial signature for Crohn's disease. Gut *66*, 813–822. https://doi.org/10.1136/gutjnl-2016-313235.
48. Mukherjee, A., Lordan, C., Ross, R.P., and Cotter, P.D. (2020). Gut microbes from the phylogenetically diverse genus Eubacterium and their various contributions to gut health. Gut Microb. *12*, 1802866. https://doi.org/10.1080/19490976.2020.1802866.
49. Sasaki, M., Schwab, C., Ramirez Garcia, A., Li, Q., Ferstl, R., Bersuch, E., Akdis, C.A., Lauener, R.; CK-CARE study group, and Frei, R., et al. (2022). The abundance of Ruminococcus bromii is associated with faecal butyrate levels and atopic dermatitis in infancy. Allergy *77*, 3629–3640. https://doi.org/10.1111/all.15440.
50. Aluwong, T., Kobo, P.I., and Abdullahi, A. (2010). Volatile fatty acids production in ruminants and the role of monocarboxylate transporters: a review. Afr. J. Biotechnol. *9*, 6229–6232.
51. Liang, J., Nabi, M., Zhang, P., Zhang, G., Cai, Y., Wang, Q., Zhou, Z., Ding, Y., and Ding, Y. (2020). Promising biological conversion of lignocellulosic biomass to renewable energy with rumen microorganisms: A comprehensive review. Renew. Sustain. Energy Rev. *134*, 110335. https://doi.org/10.1016/j.rser.2020.110335.
52. Cheng, M., McCarl, B., and Fei, C. (2022). Climate change and livestock production: A literature review. Atmosphere *13*, 140. https://doi.org/10.3390/atmos13010140.
53. Rampelli, S., Schnorr, S.L., Consolandi, C., Turroni, S., Severgnini, M., Peano, C., Brigidi, P., Crittenden, A.N., Henry, A.G., Candela, M., and Candela, M. (2015). Metagenome sequencing of the Hadza hunter-gatherer gut microbiota. Curr. Biol. *25*, 1682–1693. https://doi.org/10.1016/j.cub.2015.04.055.
54. Rampelli, S., Turroni, S., Debandi, F., Alberdi, A., Schnorr, S.L., Hofman, C.A., Taddia, A., Helg, R., Biagi, E., Brigidi, P., et al. (2021). The gut microbiome buffers dietary adaptation in Bronze Age domesticated dogs. iScience *24*, 102816. https://doi.org/10.1016/j.isci.2021.102816.
55. Pasolli, E., Asnicar, F., Manara, S., Zolfo, M., Karcher, N., Armanini, F., Beghini, F., Manghi, P., Tett, A., Ghensi, P., et al. (2019). Extensive unexplored human microbiome diversity revealed by over 150,000 genomes from metagenomes spanning age, geography, and lifestyle. Cell *176*, 649–662.e20. https://doi.org/10.1016/j.cell.2019.01.001.
56. Mukherjee, S., Seshadri, R., Varghese, N.J., Eloe-Fadrosh, E.A., Meier-Kolthoff, J.P., Göker, M., Coates, R.C., Hadjithomas, M., Pavlopoulos, G.A., Paez-Espino, D., et al. (2017). 1,003 reference genomes of bacterial and archaeal isolates expand coverage of the tree of life. Nat. Biotechnol. *35*, 676–683. https://doi.org/10.1038/nbt.3886.
57. Stewart, R.D., Auffret, M.D., Warr, A., Wiser, A.H., Press, M.O., Langford, K.W., Liachko, I., Snelling, T.J., Dewhurst, R.J., Walker, A.W., et al. (2018). Assembly of 913 microbial genomes from metagenomic sequencing of the cow rumen. Nat. Commun. *9*, 870. https://doi.org/10.1038/s41467-018-03317-6.
58. Stewart, R.D., Auffret, M.D., Warr, A., Walker, A.W., Roehe, R., and Watson, M. (2019). Compendium of 4,941 rumen metagenome-assembled genomes for rumen microbiome biology and enzyme discovery. Nat. Biotechnol. *37*, 953–961. https://doi.org/10.1038/s41587-019-0202-3.
59. Langmead, B., and Salzberg, S.L. (2012). Fast gapped-read alignment with Bowtie 2. Nat. Methods *9*, 357–359. https://doi.org/10.1038/nmeth.1923.
60. Machado, D., Andrejev, S., Tramontano, M., and Patil, K.R. (2018). Fast automated reconstruction of genome-scale metabolic models for microbial species and communities. Nucleic Acids Res. *46*, 7542–7553. https://doi.org/10.1093/nar/gky537.
61. Parks, D.H., Imelfort, M., Skennerton, C.T., Hugenholtz, P., and Tyson, G.W. (2015). CheckM: assessing the quality of microbial genomes recovered from isolates, single cells, and metagenomes. Genome Res. *25*, 1043–1055. https://doi.org/10.1101/gr.186072.114.
62. Olm, M.R., Brown, C.T., Brooks, B., and Banfield, J.F. (2017). dRep: a tool for fast and accurate genomic comparisons that enables improved genome recovery from metagenomes through de-replication. The ISME journal *11*, 2864–2868.
63. Warnes, M.G.R., Bolker, B., Bonebakker, L., Gentleman, R., Huber, W., and Liaw, A. (2016). Package 'gplots'. Various R programming tools for plotting data, 112–119.
64. Chaumeil, P.A., Mussig, A.J., Hugenholtz, P., and Parks, D.H. (2019). GTDB-Tk: a toolkit to classify genomes with the Genome Taxonomy Database. Bioinformatics. *36*, 1925–1927. https://doi.org/10.1093/bioinformatics/btz848.
65. Belcour, A., Frioux, C., Aite, M., Bretaudeau, A., Hildebrand, F., and Siegel, A. (2020). Metage2Metabo, microbiota-scale metabolic complementarity for the identification of key species. Elife *9*, e61968. https://doi.org/10.7554/eLife.61968.
66. Uritskiy, G.V., DiRuggiero, J., and Taylor, J. (2018). MetaWRAP—a flexible pipeline for genome-resolved metagenomic data analysis. Microbiome *6*, 1–13.
67. Seemann, T. (2014). Prokka: rapid prokaryotic genome annotation. Bioinformatics *30*, 2068–2069.
68. Danecek, P., Bonfield, J.K., Liddle, J., Marshall, J., Ohan, V., Pollard, M.O., Whitwham, A., Keane, T., McCarthy, S.A., Davies, R.M., et al. (2021). Twelve years of

SAMtools and BCFtools. GigaScience *10*, giab008.

69. Oksanen, J., Simpson, G.L., Blanchet, F.G., Kindt, R., Legendre, P., Minchin, P.R., and Weedon, J. (2022). Vegan: Community Ecology Package (R Foundation for Statistical Computing). 2.6–2.
70. Pignatti, S., Guarino, R., and La Rosa, M. (2017–2019). Flora d'Italia*1*, second edition, pp. 1–4.
71. Yu, Z., and Morrison, M. (2004). Improved extraction of PCR-quality community DNA from digesta and fecal samples. Biotechniques *36*, 808–812. https://doi.org/10.2144/04365ST04.
72. Turroni, S., Fiori, J., Rampelli, S., Schnorr, S.L., Consolandi, C., Barone, M., Biagi, E., Fanelli, F., Mezzullo, M., Crittenden, A.N., et al. (2016). Fecal metabolome of the Hadza hunter-gatherers: a host-microbiome integrative view. Sci. Rep. *6*, 32826. https://doi.org/10.1038/srep32826.
73. Masella, A.P., Bartram, A.K., Truszkowski, J.M., Brown, D.G., and Neufeld, J.D. (2012). PANDAseq: paired-end assembler for illumina sequences. BMC Bioinf. *13*, 31–37. https://doi.org/10.1186/1471-2105-13-31.
74. Bolyen, E., Rideout, J.R., Dillon, M.R., Bokulich, N.A., Abnet, C.C., Al-Ghalith, G.A., Alexander, H., Alm, E.J., Arumugam, M., Asnicar, F., et al. (2019). Reproducible, interactive, scalable and extensible microbiome data science using QIIME 2. Nat. Biotechnol. *37*, 852–857. https://doi.org/10.1038/s41587-019-0209-9.
75. Edgar, R.C. (2010). Search and clustering orders of magnitude faster than BLAST. Bioinformatics *26*, 2460–2461. https://doi.org/10.1093/bioinformatics/btq461.
76. Callahan, B.J., McMurdie, P.J., Rosen, M.J., Han, A.W., Johnson, A.J.A., and Holmes, S.P. (2016). DADA2: High-resolution sample inference from Illumina amplicon data. Nat. Methods *13*, 581–583. https://doi.org/10.1038/nmeth.3869.
77. Rognes, T., Flouri, T., Nichols, B., Quince, C., and Mahé, F. (2016). VSEARCH: a versatile open source tool for metagenomics. PeerJ *4*, e2584. https://doi.org/10.7717/peerj.2584.
78. Quast, C., Pruesse, E., Yilmaz, P., Gerken, J., Schweer, T., Yarza, P., Peplies, J., Glöckner, F.O., and Glöckner, F.O. (2013). The SILVA ribosomal RNA gene database project: improved data processing and web-based tools. Nucleic Acids Res. *41*, D590–D596. https://doi.org/10.1093/nar/gks1219.
79. Culhane, A.C., Thioulouse, J., Perrière, G., and Higgins, D.G. (2005). MADE4: an R package for multivariate analysis of gene expression data. Bioinformatics *21*, 2789–2790. https://doi.org/10.1093/bioinformatics/bti394.
80. Martinez Arbizu, P. (2020). pairwiseAdonis: Pairwise multilevel comparison using adonis. R package version 0.4 *1*.
81. Segata, N., Izard, J., Waldron, L., Gevers, D., Miropolsky, L., Garrett, W.S., and Huttenhower, C. (2011). Metagenomic biomarker discovery and explanation. Genome Biol. *12*, R60. https://doi.org/10.1186/gb-2011-12-6-r60.
82. Beghini, F., McIver, L.J., Blanco-Míguez, A., Dubois, L., Asnicar, F., Maharjan, S., Mailyan, A., Manghi, P., Scholz, M., Thomas, A.M., et al. (2021). Integrating taxonomic, functional, and strain-level profiling of diverse microbial communities with bioBakery 3. Elife *10*, e65088. https://doi.org/10.7554/eLife.65088.
83. Asnicar, F., Thomas, A.M., Beghini, F., Mengoni, C., Manara, S., Manghi, P., Zhu, Q., Bolzan, M., Cumbo, F., May, U., et al. (2020). Precise phylogenetic analysis of microbial isolates and genomes from metagenomes using PhyloPhlAn 3.0. Nat. Commun. *11*, 2500. https://doi.org/10.1038/s41467-020-16366-7.
84. Fiori, J., Turroni, S., Candela, M., Brigidi, P., and Gotti, R. (2018). Simultaneous HS-SPME GC-MS determination of short chain fatty acids, trimethylamine and trimethylamine N-oxide for gut microbiota metabolic profile. Talanta *189*, 573–578. https://doi.org/10.1016/j.talanta.2018.07.051.
85. Nam, S.L., Mata, A.P.d.l., Dias, R.P., and Harynuk, J.J. (2020). Towards standardization of data normalization strategies to improve urinary metabolomics studies by GC× GC-TOFMS. Metabolites *10*, 376. https://doi.org/10.3390/metabo10090376.

STAR★METHODS

KEY RESOURCES TABLE

REAGENT or RESOURCE	SOURCE	IDENTIFIER
Critical commercial assays		
DNeasy Blood & Tissue	QIAGEN	Cat#69506
NextSeq 500/550 High Output Kit v2.5 (300 Cycles)	Illumina	Cat#20024908
QIAseq FX DNA Library CDI Kit (96)	QIAGEN	Cat#180484
Chemicals		
AMPure XP magnetic beads	Beckman Coulter	Cat#A63881
Deposited data		
Human gut metagenomes	Pasolli et al. 2019[55]	http://segatalab.cibio.unitn.it/data/Pasolli_et_al.html
Bacterial and archael reference genomes	Mukherjee et al. 2017[56]	https://img.jgi.doe.gov/
Ruminant metagenomes	Stewart et al. 2018[57]	https://doi.org/10.7488/ds/2296
Ruminant metagenomes	Stewart et al. 2019[58]	Project number ENA: PRJEB31266
Alpine Ibex (Capra Ibex)	This study	Project number ENA: PRJEB70425
Software and algorithms		
bowtie2 2.3.4.3	Langmead et al. 2012[59]	https://github.com/BenLangmead/bowtie2
CarveMe 1.5.1	Machado et al. 2018[60]	https://github.com/cdanielmachado/carveme
CheckM 1.2.0	Parks et al. 2015[61]	https://github.com/Ecogenomics/CheckM
dRep 3.2.2	Olm et al. 2017[62]	https://github.com/MrOlm/drep
gplots 3.1.3 r package	Warnes et al., 2016[63]	https://CRAN.R-project.org/package=gplots
GTDB-Tk 2.1.0	Chaumeil et al. 2022[64]	https://github.com/Ecogenomics/GTDBTk
Metage2metabo 1.5.0	Belcour et al. 2020[65]	https://github.com/AuReMe/metage2metabo
Metawrap 1.3.2	Uritskiy et al. 2018[66]	https://github.com/bxlab/metaWRAP
Prokka 1.14.6	Seemann 2014[67]	https://github.com/tseemann/prokka
R Software 4.2.0	R Software	www.r-project.org
Samtools 1.10	Bonfield et al. 2021[68]	https://github.com/samtools/samtools
vegan 2.6–2 r package	Oksanen et al. 2022[69]	https://CRAN.R-project.org/package=vegan

RESOURCE AVAILABILITY

Lead contact

Further information and request for resources and reagents should be directed to and will be fulfilled by the lead contacts, Marco Candela (marco.candela@unibo.it).

Materials availability

This study did not generate new unique reagents.

Data and code availability

- High-quality reads from the samples sequenced in this study were deposited in the European Nucleotide Archive under the project accession number ENA: PRJEB70425.
- Ruminant and human metagenomes derived from 4 previously published studies available in public repositories (see key resources table for references).
- This paper does not report original code.
- Any additional information required to reanalyze the data reported in this paper is available from the lead contact upon request.

EXPERIMENTAL MODEL AND STUDY PARTICIPANT DETAILS

Shotgun metagenomes

Alpine ibex (*Capra ibex*) metagenome datasets used in this study are sequenced in this study (see data and code availability section for further details), other ruminant and human metagenomes derived from 4 previously published studies available in public repositories (see method details and key resources table for the respective references).

METHOD DETAILS

Study site and sampling procedure

A total of 86 fecal samples were collected at Stelvio National Park (Lombardia, Italy) from an equal number of Alpine ibex specimens, which were followed and observed until defecation. When possible, surface soil and grass samples were also collected in the proximity, for a total of 111 samples (i.e., 86 ibex feces, 17 soil and 8 grass samples). Samples were collected at two different nearby sites, namely "Passo del Gavia" (46°20'04.1"N/10°29'15.4"E) and "Valle del Braulio" (46°31'03.4"N/10°24'42.8"E), across three different seasons, namely spring (16th, 17th and 18th June 2020), summer (3rd, 4th and 5th August 2020) and fall (1st and 2nd October 2020) (Figure S1). A schematic summary of the sample distribution across the two sites and the three timepoints is provided in Table S1. All samples were collected using sterile gloves, placed in sterile plastic tubes, and kept frozen at −20°C until microbial DNA extraction. The mean values of snow on the ground (cm) for the sampling year were retrieved from the meteorological station Valdisotto Oga S. Colombano (SO, ARPA Lombardia), which is located at an altitude of 2300 m and collects detailed measurements almost every 30 min. Data from July to June of the subsequent year (from 1992 to 2022) are reported in Figure S2. Coordinates of sampling sites were uploaded in the Italian Geoportale Nazionale (http://www.pcn.minambiente.it/viewer/index.php?services=progetto_natura), managed by the Ministry of Environment and providing different kinds of spatial data. In particular, a map of plant alliances of the sampling sites was retrieved form the portal. Plant species characterizing the identified phytosociological synthaxa were then inferred according to Prodromo della Vegetazione Italiana (https://www.prodromo-vegetazione-italia.org). Each species was assigned to a Raunkiaer's life form (chamaephytes, geophytes, hemicryptophytes, phanerophytes and therophytes) using Pignatti et al.[70]

Microbial DNA extraction, 16S rRNA amplification and sequencing

Total microbial DNA was extracted from approximately 0.25 g of each of the 111 samples, i.e., ibex feces, soil, and grass. DNA extraction from fecal samples was performed using the DNeasy Blood & Tissue Kit (QIAGEN, Hilden, DEU) with a modified protocol.[71] In brief, fecal material was added with four 3-mm glass beads and 0.5 g of 0.1-mm zirconia beads (BioSpec Products, Bartlesville, OK, USA), and the homogenization step was performed three times using a FastPrep instrument (MP Biomedicals, Irvine, CA, USA) at 5.5 m/s for 1 min. Samples were then heated at 95°C for 15 mins. DNA from soil and grass was extracted using the DNeasy PowerSoil Kit (QIAGEN) following the manufacturer's instructions with a minor modification: a FastPrep instrument (MP Biomedicals) was used for the homogenization step as described above. DNA was quantified using a NanoDrop ND1000 spectrophotometer (NanoDrop Technologies, Wilmington, DEU). PCR was performed in a final volume of 50 µL containing genomic DNA (25 ng), 2X KAPA HiFi HotStart ReadyMix (Roche, Basel, CHE) and 200 nmol/L of 341F and 785R primers carrying Illumina overhang adapter sequences for amplification of the V3-V4 hypervariable regions of the 16S rRNA gene. The PCR thermal cycle consisted of an initial denaturation (95°C for 3 mins), followed by 25 cycles of denaturation (95°C for 30 s), primer annealing (55°C for 30 s) and DNA extension (72°C for 30 s); the entire reaction was completed with a final extension step (72°C for 5 mins).[72] PCR amplicons were then cleaned up using Agencourt AMPure XP magnetic beads (Beckman Coulter, Brea, CA, USA). Indexed libraries were prepared by limited-cycle PCR using Nextera technology and purified as above. Finally, the libraries were quantified using a Qubit 3.0 fluorimeter (Invitrogen, Waltham, Massachusetts, USA), normalized to a concentration of 4 nM and pooled in a single Eppendorf tube. The pool was denatured with 0.2 N NaOH and diluted to a final concentration of 4.5 pM with a 20% PhiX control. Sequencing was performed on an Illumina MiSeq platform using a 2 x 250 bp paired-end protocol, according to the manufacturer's instructions (Illumina, San Diego, CA, USA).

Metabarcoding bioinformatics and biostatistics

Raw sequences were analyzed using a pipeline combining PANDAseq[73] and QIIME 2.[74] High-quality reads (min/max length = 350/550 bp) were retained using the "fastq filter" function of the Usearch11 algorithm[75] and then binned into amplicon sequence variants (ASVs) using DADA2.[76] The VSEARCH algorithm[77] and the SILVA database (December 2017 release)[78] were used for taxonomic classification. All unassigned and eukaryotic sequences were discarded. Overall, an average sequencing depth of 10,725 ± 2,871 (mean ± SD) high-quality reads per sample was obtained, resulting in a total of 20,592 ASVs. Alpha-diversity was assessed using three different metrics, namely Faith's Phylogenetic Diversity (PD whole tree), the number of observed ASVs and the Shannon index. Beta-diversity was assessed using Bray-Curtis distances.

Statistical analyses were performed using R software (https://www.r-project.org/), v. 4.2.0, implemented with the packages "Made4",[79] "vegan"[69] (https://cran.r-project.org/web/packages/vegan/index.html), "pairwiseAdonis"[80] and "gplots"[63] (https://cran.r-project.org/web/packages/gplots/index.html). Data separation in the PCoAs was assessed using a permutation test with pseudo-F ratio (functions "adonis" in the vegan package and function "pairwiseAdonis" in the homonymous package). A procrustean randomized test (function "protest" in the vegan package) was performed to highlight significant relationship between microbiome and metabolomic distance matrices. The Kruskal-Wallis test among groups was used to assess significant differences in alpha-diversity (calculated on taxonomical annotation). P-values were corrected for multiple testing, when necessary, using the Benjamini-Hochberg method, with a false discovery rate (FDR) ≤ 0.05 considered

statistically significant. Linear discriminant analysis (LDA) effect size[81] (LEfSe) was used to identify discriminant genera across the three time-points ($p \leq 0.05$). The online Galaxy Version interface (https://huttenhower.sph.harvard.edu/galaxy/, last accessed September 2023) was used.

Shotgun metagenomics sequencing

A subset of representative 12 Alpine ibex fecal samples (six per site, including two per season) was selected for shotgun metagenomic sequencing. The QIAseq FX DNA library kit (QIAGEN) was used for DNA library preparation according to the manufacturer's instructions. Briefly, 450-bp size, end-repaired and A-tailed fragments were generated by fragmenting 100 ng of each DNA sample using FX enzyme mix with the following thermal cycle: 4°C for 1 min, 32°C for 8 mins and 65°C for 30 mins. DNA samples were then incubated at 20°C for 15 mins to perform adapter ligation in the presence of DNA ligase and Illumina adapter barcodes. Agencourt AMPure XP magnetic beads (Beckman Coulter) were used for purification, followed by library amplification with a 10-cycle PCR and a further purification step. Samples were then pooled at an equimolar concentration (4 nM) to obtain the final library. Sequencing was performed on an Illumina NextSeq platform using a 2 × 150 bp paired-end protocol, following the manufacturer's instructions (Illumina).

Metagenomics bioinformatics and biostatistics

Raw reads were filtered for eukaryotic host DNA using bmtagger software and *Capra ibex* (NCBI GenBank accession: GCA_006410555.1) as a reference. After this filtering step, reads were processed with trimBWAstyle (https://github.com/genome/genome/blob/master/lib/perl/Genome/Site/TGI/Hmp/HmpSraProcess/trimBWAstyle.usingBam.pl) for quality trimming (quality score above 20) and length drop with default parameters. Duplicates were estimated and removed using the Picard tool EstimatedLibraryComplexity (v. 1.71). A total of 61 million high-quality microbial paired-end reads were retained, with an average of 5.2 ± 1.0 (mean ± SD) million reads per sample. The resulting reads were used to obtain a general functional annotation for each sample, using HUMAnN v. 3.0.1.[82] The output tables were then normalized using humann_renorm_table with the following parameter "—units cpm". The resulting tables were merged and then processed by removing the UNMAPPED ID and converting the UniRef90 classification into the KEGG Orthology (KO) classification. This final table was used to compute alpha-diversity indices (Shannon, Simpson, and observed features) and beta-diversity based on Bray-Curtis distances. Data separation in the Bray-Curtis-based PCoA was assessed in R using a permutation test with pseudo-F ratio (function "adonis" in the vegan package and function "pairwiseAdonis" in the homonymous package). The Kruskal-Wallis test among groups was used to assess significant differences in alpha-diversity, with P-values corrected for multiple testing as previously described. In parallel, high-quality reads were assembled using metaspades.py (v. 3.15.3) with default parameters. Each assembly was annotated using prokka[67] (v. 1.14.6) with default parameters and "—addgenes" to retrieve all classes of Carbohydrate-Active enZYmes (CAZymes), according to the latest version of the online CAZy database, namely glycoside hydrolases (GHs, EC 3.2.1.-), glycosyl transferases (GTs, EC 2.4.x.y), polysaccharide lyases (PLs, EC 4.2.2.-), carbohydrate esterases (CEs) and auxiliary activities (AAs) enzymes. Using prokka output files, open reading frames (ORFs) for each CAZyme were retrieved and used to build a reference database, dereplicated at 90% similarity and used to assess the abundance of each CAZyme in our samples. Alignment was performed using Bowtie2 v. 2.3.4.3[59] with the parameter "–end-to-end –very-sensitive"; the number of aligned reads for each sample was then retrieved using Samtools v. 1.16.[68] Reads per kilobase of gene per million reads mapped (RPKMs) in each sample and for each gene were calculated by summing the number of reads of all mapped ORFs and processed as follows:

$$\frac{Total\ reads\ mapped\ to\ gene}{Total\ reads\ *\ Mean\ Gene\ length} * 10^9$$

The abundance table, in terms of RPKMs, of each CAZyme family identified in our dataset was used to plot a heatmap of the CAZymes families involved in the catabolism of plant polysaccharides, assigned to the corresponding functional classes, using the heatmap.2 function in R. The Spearman distance and the ward.D2 method were used to cluster the different samples according to the obtained CAZymes abundances. The heatmap represents the Z-score of the identified CAZymes families, with clustering performed for samples. The RPKMs abundance table of the CAZymes families assigned to a specific functional class was also used to calculate alpha-diversity, using the number of observed features, the Simpson index, and the Shannon index.

Metagenome-Assembled Genomes (MAGs) reconstruction

Assemblies from each sample were used to construct Metagenome-Assembled Genomes (MAGs) using the metawrap binning module (metawrap version 1.3.2[66]). Only MAGs with completeness > 50% and contamination < 5%, as assessed through the checkm lineage_wf workflow,[61] were retained. All retrieved high-quality MAGs were then dereplicated into species-level genome bins (SGBs) using the dRep dereplicate command (dRep v. 3.2.2[62]) and the following parameters: "–ignoreGenomeQuality -pa 0.9 -sa 0.95 -nc 0.30 -cm larger -centW 0". The taxonomic classification of SGBs was performed using the gtdbtk classify_wf workflow with default parameters,[64] while the abundance of each SGB in each sample was obtained using the metawrap quant_bins module (metawrap v. 1.3.2). The SGBs abundance table was used to construct a presence/absence table of each SGB across samples. A phylogenetic tree including all SGBs was then built by using phylophlan[83] with the parameters "–diversity low –fast –min_num_markers 79", and used to measure UniFrac distances between samples, which were plotted in a Principal Coordinates Analysis (PCoA) graph. Finally, the SGBs were compared, using MinHash sketches implemented in the mash tool (v. 2.3), with 8,217 genomes from three of the largest ruminant gut metagenomic datasets,[10,57,58] with the Genomic Encyclopedia

of Bacteria and Archaea (GEBA) collection[56] and with 4,930 SGBs previously identified in a study describing the gut microbiome of different human individuals across age, geography and lifestyle.[55]

Genome-scale metabolic models for the degradation of plant food substrates

Microbiome-scale metabolic models for the identification of key SGBs involved in the degradation of plant food substrates, such as cellulose, hemicellulose, pectin, and lignin, were obtained using CarveMe[60] and Metage2Metabo.[65] Specifically, CarveMe was applied to each SGB, grouped by timepoint, using the default options, to build the specific genome-scale metabolic model (GSMM) for each SGB. Metage2Metabo was then used with the parameter "metacom" to build a single metabolic network combining all the GSMMs by timepoint and retrieving the list of the minimal communities of SGBs essential for the degradation of plant components. The pipeline was repeated using as input the set of GSMMs divided by timepoint and considering the 4 main plant biopolymers.

Metabolomics

All fecal samples underwent two kinds of analytical characterization: SCFAs (Short Chain Fatty Acids) and BCFAs (Branched Chain Fatty Acids) quantitation through head space-solid phase microextraction (HS-SPME-GC-MS) and untargeted metabolomic analysis with liquid chromatography-high resolution mass spectrometry (LC-HRMS) analysis.

Reagents, materials and solutions

All standards (purity > 99%) for acetic, propionic, butyric, isobutyric, valeric, isovaleric and d8-butyric acids (d8-BA) were provided by Sigma-Aldrich (Milan, ITA). Perchloric acid ($HClO_4$) 70 was also provided by Sigma-Aldrich. MILLEX GP syringe filter, 0.22 μm in pore size, with Polyethesulfone (PES) membrane were provided by Millipore corp. (Bedford, MA). UHPLC-MS grade acetonitrile, UHPLC-MS grade methanol and water were provided by VWR Chemicals (Radnor, PA, USA). LC-MS grade formic acid was purchased from Carlo Erba Reagents S.r.l. (Milan, ITA). The manual holder and the commercially available SPME fibers 75 μm Carboxen™/polydimethylsiloxane (CAR/PDMS) were purchased from Supelco (Bellefonte, PA, USA). Prior to first use, the SPME fiber was conditioned for 60 minutes at 300°C as per manufacturer's instructions. Individual acid stock solutions were prepared at a concentration of 1,000 ppm (μg/mL) by diluting 20 μL of acid with milliQ water in a 20-mL volumetric flask. Individual standard solutions were prepared by diluting the stock solution to final concentrations of 5, 10, 25, 50 and 100 ppm. A stock solution for internal standard (d8-BA) at a concentration of 10 mg/mL was obtained by diluting 95.2 μL of acid with H_2O in a 10-mL volumetric flask. From this stock solution, a working solution with a final concentration of 0.5 mg/mL was obtained by successive dilution with milliQ water. LC-MS analysis was performed on an Eksigent M5 MicroLC system (Sciex, Concord, Ontario, Canada) coupled to a TripleTOF 6600+ mass spectrometer with OptiFlow Turbo V Ion Source (Sciex).

HS-SPME GC-MS analysis for SCFAs and BCFAs

Solid-liquid extraction was performed as a preliminary clean-up. A perchloric acid solution (10% v/v in water) was added to frozen aliquots of fecal samples to a final concentration of 250 mg/mL. The resulting solutions were centrifuged at 15,000 rpm for 10 minutes at 4°C. After centrifugation, the supernatant was collected in a 1.5-mL glass vial and stored at -20°C. For HS-SPME analysis, 50 μL of fecal sample solution were added to 450 μL of H_2O and 10 μL of IS solution in a 4-mL glass vial, which was then capped with a pierceable septum cap. Prior to extraction, the vials containing the samples were heated at 70°C for 10 minutes under continuous stirring at 270 rpm using a poly(tetrafluoroethylene)-coated magnetic stir bar. After thermal conditioning, the septum of the vial was pierced with the needle of the SPME device and the fiber was exposed approximately 10 mm above the solid sample, allowing extraction of the analytes for 30 minutes. The optimized temperatures and times were slightly modified as pointed out by Fiori and colleagues in a previously published article.[84] After extraction, the fiber was retracted into the protective sheath, removed from the headspace glass vial and transferred without delay into the injection port of the gas chromatograph/mass spectrometer. The fiber was thermally desorbed in the injection port at 250°C for 2 minutes and the GC/MS run was started. To thermally clean the SPME fiber, it was left in the injection port for an additional 8 minutes after complete desorption of the analytes.

GC-MS analysis was carried out on a TRACE GC 2000 Series (ThermoQuest CE Instruments, Austin, TX, USA) gas chromatograph, interfaced with Trace ITQ MS (ThermoQuest CE) mass detector with 3D ion trap analyzer, operating in EI mode (70 eV). The capillary GC column was a Phenomenex ZB-WAX (30 m x 0.25 mm ID, 0.15 μm film thickness). Helium (He) was used as carrier gas at a flow rate of 1.0 mL/min. A temperature program was adopted: initial temperature was 40°C (hold time: 5 mins), then temperature ramped by 10 °C/min to 220°C (hold time: 5 mins). The temperatures of the transfer line and ionization source were maintained at 250°C and 200°C, respectively. The GC was operated in splitless mode. Mass spectra were recorded in full scan mode (34-200 amu) to collect total ion current chromatograms. Quantitation was carried out using the extracted ion chromatograms by selecting qualifier and quantifier fragment ions of the studied analytes: 43 and 60 amu for AA, 55 and 73 amu for PA, 55 and 77 amu for iBA, 60 and 87 amu for iVA, 60 and 73 amu for BA and VA, 63 and 77 amu for d8-BA.

LC-HRMSMS untargeted metabolomics

For metabolome analysis, approximately 200 mg of homogenized fecal samples were extracted by the addition of three equivalents (weight/Vv) of methanol, followed by vortex-mixing for 3 seconds and sonication for 10 minutes. The samples were then centrifuged at 14,000 rpm for 10 minutes at 4°C, and the supernatant was collected and filtered through 0.22-μm PES membranes. The obtained extracts were stored

at -80°C until further analysis. In order to avoid bias, all experimental samples were randomized before sample preparation and before analytical run. Interpooled Quality Control samples (QCs) were prepared by pooling together equal aliquots (10 μL) from each sample before extraction and underwent the same treatment as experimental samples. Before injection, each methanol extract was diluted in a 1:10 ratio with Milli-Q water.

LC-MS analysis was performed on an Eksigent M5 MicroLC system (Sciex) coupled to a TripleTOF 6600+ mass spectrometer with OptiFlow Turbo V Ion Source (Sciex). Analyses were carried out in both positive and negative ionization, with the column temperature set at 35°C. In brief, 5 μL from each sample were loaded onto a Phenomenex Luna Omega Polar C18 100 × 1.0 mm I.D. 1.6 μm 100 Å. Before the first sample injection, the same QC sample was injected repeatedly, for a total of 10 times, to allow for system equilibration and conditioning. Chromatographic separation occurred in 25 minutes at a constant flow rate of 30 μL/min. The gradient elution program was as follows: 0-2 minutes, 0.2% eluent B; 2-5 minutes, 0.2-15% eluent B; 5-15 minutes, 15-70% eluent B; 15-18 minutes, 70-98% eluent B; 18-20 minutes, 98% eluent B; 20-22 minutes, 98-0.2% eluent B; 22-25 minutes, 0.2% eluent B. Equilibration time between chromatographic runs was 3 minutes. Mobile phase A consisted of 0.1% formic acid and mobile phase B was acetonitrile/0.1% formic acid. IonSpray voltage (ISV) was 5,000 V and Curtain Gas supply pressure (CUR) was 30 PSI; nebulizer and heater gas pressures were set at 30 and 40 PSI, respectively. The ion spray probe temperature was 300°C. Declustering potential was 80 V. Analyses were carried out using a collision energy of 40 eV. Sample analyses were performed in Data Independent Acquisition mode (SWATH-MS: Sequential Window Acquisition of All Theoretical Mass Spectra). The variable SWATH windows used for acquisition were obtained through the SWATH Variable Window Calculator app (Sciex). The software employs the m/z density histogram constructed from the TOF MS analysis to equalize the density of the precursors in each window across the m/z range. The overlap between windows was 1 Da. PepCal Mix (Sciex) was used to ensure steady MS and MSMS calibrations during the whole analysis timeframe.

Data analysis

SWATH raw data files were viewed using PeakView 2.2 (AB sciex). Peak picking (minimum spectral peak width of 10 ppm, minimum peak width of five scans), alignment, filtering (intensity threshold of 10,000 cps, removal of features detected in less than 50% of samples) and annotation were performed using SCIEX OS. Untargeted metabolomic analysis was based on all ion features in the SWATH-MS/MS data after peak finding, alignment and filtering. Metabolites eluted close to the solvent front (< 1 min) were excluded. Fatty acids abundances were represented by boxplots. The Kruskal-Wallis test among groups followed by post-hoc Wilcoxon rank-sum test between pairs of groups were used to assess significant differences in fatty acids abundances, with P-values corrected for multiple testing as previously described. The untargeted metabolomic data were normalized according to the Total Peak Area method, i.e., each peak area was normalized to the sum of the areas of all detected peaks in each sample.[85] The normalized table, based on negative ionization, was then used to calculate the relative abundance of each metabolite in each sample. The resulting relative abundance table was used in R as input to compute the PCoA, based on the Bray-Curtis distances between samples, using the "vegdist" function from the vegan package.